


# BDNF signaling contributes to oral cancer pain in a preclinical orthotopic rodent model

Leah Chodroff, MS, MD<sup>1,2</sup>, Michelle Bendele, BS<sup>1</sup>,  
Vanessa Valenzuela, BS<sup>1</sup>, Michael Henry, DDS, PhD<sup>1</sup> and  
Shivani Ruparel, MS, PhD<sup>1</sup>

Molecular Pain  
Volume 12: 1–17  
© The Author(s) 2016  
Reprints and permissions:  
sagepub.co.uk/journalsPermissions.nav  
DOI: 10.1177/1744806916666841  
mpx.sagepub.com  


## Abstract

The majority of patients with oral cancer report intense pain that is only partially managed by current analgesics. Thus, there is a strong need to study mechanisms as well as develop novel analgesics for oral cancer pain. Current study employed an orthotopic tongue cancer model with molecular and non-reflexive behavioral assays to determine possible mechanisms of oral cancer pain. Human oral squamous cell carcinoma cells line, HSC2, was injected into the tongue of male athymic mice and tumor growth was observed by day 6. Immunohistological analyses revealed a well-differentiated tumor with a localized immune response and pronounced sensory and sympathetic innervation and vascularization. The tumor expressed TMPRSS2, a protein previously reported with oral squamous cell carcinoma. ATF3 expression in trigeminal ganglia was not altered by tumor growth. Molecular characterization of the model demonstrated altered expression of several pain-related genes, out of which up-regulation of BDNF was most striking. Moreover, BDNF protein expression in trigeminal ganglia neurons was increased and inhibition of BDNF signaling with a tyrosine kinase B antagonist, ANA-12, reversed pain-like behaviors induced by the oral tumor. Oral squamous cell carcinoma tumor growth was also associated with a reduction in feeding, mechanical hypersensitivity in the face, as well as spontaneous pain behaviors as measured by the conditioned place preference test, all of which were reversed by analgesics. Interestingly, injection of HSC2 into the hindpaw did not reproduce this spectrum of pain behaviors; nor did injection of a colonic cancer cell line into the tongue. Taken together, this orthotopic oral cancer pain model reproduces the spectrum of pain reported by oral cancer patients, including higher order cognitive changes, and demonstrates that BDNF signaling constitutes a novel mechanism by which oral squamous cell carcinoma induces pain. Identification of the key role of tyrosine kinase B signaling in oral cancer pain may serve as a novel target for drug development.

## Keywords

BDNF, oral cancer pain, orthotopic model, tongue cancer

Date received: 13 June 2016; revised: 2 August 2016; accepted: 3 August 2016

## Introduction

Most head and neck cancers (HNC) are of squamous cell origin<sup>1,2</sup> that develop in the throat, larynx, nose, sinuses, or the mouth. Pain is reported in 70–85% of these patients and is ranked as the top of all symptoms of HNC.<sup>3</sup> Indeed, pain is typically the symptom that prompts patients to seek initial treatment.<sup>4–6</sup> Several groups have reported a greater prevalence of pain in HNC patients compared to other cancer types.<sup>7,8</sup> This may be partly due to specific properties of head and neck tumors, or to distinguishing characteristics of

<sup>1</sup>Department of Endodontics, University of Texas Health Science Center at San Antonio, San Antonio, TX, USA

<sup>2</sup>Department of Surgery, University of Texas Health Science Center at San Antonio, San Antonio, TX, USA

### Corresponding author:

Shivani Ruparel, Department of Endodontics, University of Texas Health Science Center at San Antonio, 7703 Floyd Curl Drive, San Antonio, TX 78229, USA.

Email: ruparels@uthscsa.edu



orofacial tissues such as the oropharynx, trigeminal afferent neurons, or medullary dorsal horn circuitry.<sup>9</sup> Among all HNC subtypes, patients with a primary lesion in the oral cavity, particularly either in the tongue or the floor of the mouth, report the greatest magnitude of pain.<sup>10</sup> Oral cancer patients typically experience pain at the primary site of the tumor development,<sup>11,12</sup> even when the tumor is still quite small in size, and pain intensity often increases as the tumor progresses. Patients experience spontaneous pain and mechanical allodynia, as well as function-related pain such as dysphagia and difficulty in chewing and swallowing.<sup>10,11,13</sup> Additionally, patients also experience referred pain such as in the face, dental pain, ear, gingiva, and the neck.<sup>10</sup> Patients can be initially treated with non-narcotic medications such as NSAIDs; however, as the tumor progresses, treatment becomes inadequate, with patients subsequently requiring opiates that are associated with both side effects and tolerance.<sup>10,13–16</sup> Moreover, reports indicate that HNC patients have the highest opioid reescalation index, suggesting that these patients develop opioid tolerance faster than other cancer types.<sup>17</sup> Thus, pain due to oral cancers, in particular, pain due to oral squamous cell carcinomas (OSCC), represents a significant problem for management.

Despite the well-recognized prevalence of pain in oral cancer patients, there is a large gap in knowledge regarding the specific mechanisms responsible for oral tumor-related pain. Here, we demonstrate the importance of an orthotopic model by comparing the behavioral phenotype of mice after injection of the OSCC cell line, HSC2, into the tongue, versus HSC2 injected into the hindpaw or injection of a colonic cancer line into the tongue. These findings extend the work of other investigators<sup>13,18–22</sup> by demonstrating that this *in vivo* orthotopic model of intraoral OSCC pain reproduces the anatomical, molecular and pain phenotype observed in OSCC patients. Molecular characterization of this *in vivo* model demonstrated that BDNF was strikingly up-regulated in the V3 region of TG neurons, upon tumor growth. Despite this, BDNF signaling has not been studied for oral cancer pain, till date. Therefore, using this orthotopic model, we demonstrate a novel role of BDNF signaling via the tyrosine kinase B (TrkB) receptor in mediating oral cancer pain. The BDNF/TrkB axis has been reported to be overexpressed in HNC and has been implicated in preventing apoptosis, promoting epithelial-to-mesenchymal transition (EMT) and conferring chemoresistance.<sup>23–25</sup> Targeting BDNF signaling with novel analgesics for treatment may therefore allow reversal of cancer-induced pain, prevent tumor progression as well as inhibit chemoresistance, collectively leading to improved quality of life of a cancer patient.

## Methods

### Cell lines

The human OSCC cell line, HSC2, was purchased from Health Science Research Resources Bank, Japan. The cell line was cultivated and maintained in Dulbecco's minimal essential medium (DMEM, Life Technologies, Carlsbad, CA) supplemented with glutamine, penicillin/streptomycin, and 10% fetal bovine serum. Two control cell lines were also studied. An immortalized human normal oral keratinocyte (NOK) cell line, OKF6-TERT2, was kindly provided by Dr. Cara Gonzales of UTHSCSA and maintained in keratinocyte serum-free media (Life Technologies, Carlsbad, CA) supplemented with 25 µg/ml bovine pituitary extract (BPE), 0.2 ng/ml epidermal growth factor (EGF), and 0.4 µM calcium chloride and penicillin/streptomycin. The human colon cancer cell line, HT29, was obtained from ATCC (Manassas, VA, USA) and maintained in RPMI 1640 (ATCC, Manassas, VA) supplemented with penicillin/streptomycin and 10% fetal bovine serum.

### Animals

The animal protocol was approved by the UTHSCSA IACUC and conforms to IASP guidelines. Six- to eight-week-old adult inbred Balb/c male athymic nude mice (Charles River, Wilmington, MA, USA) were used for all experiments. Animals were housed for at least four days prior to the start of any experiments.

### Drugs

Indomethacin was purchased from Sigma Aldrich (St. Louis, MO, USA). The drug was diluted in 5% DMSO/DPBS and administered at a dose of 5 mg/kg. Morphine was obtained from Henry Schein (Melville, NY, USA) and tramadol obtained from Sigma Aldrich (St. Louis, MO, USA). Both drugs were diluted in Dulbecco's PBS (DPBS) and administered at doses of 3 mg/kg and 20 mg/kg, respectively. The TrkB receptor antagonist, ANA-12<sup>26</sup> was purchased from Sigma Aldrich (St. Louis, MO, USA) and diluted in 10% DMSO/2% Tween-20/DPBS and injected at a dose of 1 mg/kg. Drugs were administered by i.p. injections.

### *In vivo* orthotopic xenograft model

We adopted this model from the pioneering work of Schmidt and colleagues.<sup>19–21,27</sup> HSC2 cells were harvested in growth media and prepared at a concentration of  $3.5 \times 10^5$  cells/50 µL. Volume of injection was selected based on previously published literature.<sup>19,20,28</sup> Mice were anesthetized using 2% isoflurane and 50 µl was injected into the ventral tongue over a 30-s period

**Table 1.** Antibodies used in immunohistochemical analysis.

Primary Antibody	Dilution	Company	Secondary Antibody
Anti-TMPRSS2	1:200	Abcam (MA, USA)	Goat anti-rabbit 568
Anti-human mitochondrial	1:20	Millipore (MA, USA)	Goat anti-mouse 488
Anti-CGRP	1:300	Sigma-Aldrich (MO, USA)	Goat anti-rabbit 568
Anti-NFH	1:1000	Abcam (MA, USA)	Goat anti-chicken 633
Anti-CD31	1:100	BD Pharmigen (CA, USA)	Goat anti-rat 488
Anti-Tyrosine Hydroxylase (TH)	1:400	Pel-Freeze (AR, USA)	Goat anti-rabbit 568
Anti-VonWillibrand Factor (vWF)	1:2000	Dako (CA, USA)	Goat anti-rabbit 568
Anti-ATF3	1:2000	Santa Cruz Biotechnology (TX, USA)	Goat anti-rabbit 568
Anti-BDNF	1:50	Santa Cruz Biotechnology (TX, USA)	Goat anti-Rabbit 568

using a 25-gauge needle. Control groups consisted of injection of NOK cells or HT29 colon cancer cells into the tongue, or HSC2 cells injected intraplantar (i.pl.) into the hindpaw. Following injection, animals were immediately placed in warm bedding and allowed to recover. Body weights were determined every three days post-inoculation.

### Histology

Mice were injected with HSC2 cells or NOK cells into the tongue and at day 9 post-inoculation, animals were euthanized and the tongues removed. Tissues were fixed, cryopreserved, embedded in paraffin, and 15  $\mu$ m transverse sections were stained with hematoxylin and eosin (H&E). Sections were evaluated, and images were obtained with a Nikon D-Eclipse light microscope. Images were taken at 2 $\times$ , 10 $\times$ , and 60 $\times$  magnifications using fixed acquisition parameters across all groups and images presented are unaltered from that initially taken.

### Immunohistochemistry

Mice were deeply anesthetized with an i.m. injection of ketamine (75 mg/kg) and dexmedetomidine (1 mg/kg), and transcardially perfused with 100 ml of 0.9% saline followed by 200 ml of fixative consisting of 4% paraformaldehyde (PFA) in 0.1 M phosphate buffer (PB). The trigeminal ganglia (TG) and tongue were removed, post-fixed for 20 min, rinsed in PB and placed in cold 0.1 M PB with 30% sucrose overnight. Tissues were embedded in Neg-50 (Richard Allan, Kalamazoo, MI, USA) and sectioned in the horizontal plane at 25  $\mu$ m with the use of a cryostat. Sections were placed onto Superfrost Plus slides (Fisher Scientific, Waltham, MA, USA), dried and stored at  $-20^{\circ}\text{C}$  until stained. Immunostaining was performed as described previously.<sup>29</sup> Briefly, tissue sections were permeabilized and blocked for non-specific protein binding with blocking solution consisting of 4%

normal goat serum (Sigma, St. Louis, MO), 2% bovine gamma-globulin (Sigma-Aldrich, St. Louis, MO) and 0.3% Triton X-100 (Fisher Scientific) in PBS for 90 min prior to incubation with primary antibodies in blocking solution for 16 h. Table 1 lists the antibodies, dilutions, and sources used in this study. Sections were rinsed with PBS, incubated in secondary antibody in blocking solution for 90 min, rinsed in PBS and H<sub>2</sub>O, dried and coverslipped with Vectashield. Secondary antibodies were purchased from Molecular Probes, Eugene, OR, USA. Nuclei were stained either with DAPI or TO-PRO-3 iodide (1:5000, Invitrogen, Carlsbad, CA, USA). All immunostaining procedures were performed at room temperature. Sections were evaluated and images obtained with a Nikon Eclipse 90i microscope equipped with a C1si laser scanning confocal imaging system. Multiple images were acquired of tongues and the V3 region of ipsilateral TGs using three different sections from three individual animals for each antibody combination with a 20 $\times$  objective and identical laser gain settings. Images were taken using fixed acquisition parameters across all groups and were unaltered from that initially taken.

For quantitative analysis, TG sections were collected at day 9 post-inoculation from four individual animals in each group, stained and imaged all at once at identical gain settings. Quantitation was achieved using NIS Elements software by counting total number of neurons in the V3 region of the TG tissue in each image as well as number of neurons above threshold for positive BDNF expression in the V3 area. Quantification was performed by a blinded experimenter. Data are represented as mean of percent of BDNF positive neurons for each animal for each group. A total of 350–550 neurons per animal were counted.

### Behavioral testing

OSCC patients often report difficulty in eating, referred pain, and spontaneous pain. Three behavioral assays

were employed to evaluate whether this orthotopic model reproduces this spectrum.

**Feeding behavior.** Mice were food deprived for 18 h and then injected with vehicle. Each mouse was then placed in an individual cage, without any bedding, and allowed to freely feed for 1 h on a pre-measured amount of standard chow. At the end of an hour, the amount of food intake was determined by calculating the difference (in g) from the initial amount and the remaining amount of food. Spillage of food and crumbs in the cages was collected to calculate total amount of food remaining. Because feeding was measured only for an hour, only a few (approx. 3–4) feces pellets or drops of urine was seen in the cages which was easily separated or removed before collecting the spilled crumbs. Mice were continued to be food deprived for an additional 5 h and then injected with a test drug and allowed to feed for 1 h. Water was available to the animals at all times. Baseline measurements were taken prior to cell inoculation, and then on days 4, 7, 9, and 14 post-inoculation. Although automated feeding assays have been developed,<sup>19</sup> this repeated measures design was selected to minimize the number of animals with tumor pain and preliminary studies demonstrated that sequential injection of vehicle produced no significant difference in feeding between the first and second session.

**Von Frey testing.** To evaluate referred mechanical pain, von Frey filaments were applied to the V2 trigeminal division (i.e., vibrissal pad) at nine days after injection of the tumors into the V3 trigeminal division (i.e., tongue). As previously described,<sup>30</sup> unrestrained mice were habituated to stand on the experimenter's hand who was wearing a latex-free glove. Animals were also habituated to Von Frey testing by applying the lowest force for five times, one day prior to experimentation. Animals were then injected with vehicle i.p. and 30 min later, a sequential series of calibrated von Frey filaments (bending forces ranging from 0.78 to 588 mN) were applied to the vibrissal pad. Head withdrawal, face swipe, or grimace were considered a positive response. Each force was applied five times at intervals of 3–5 s. Animals were then returned to their cages and 4 h later injected with the test drug and re-tested with von Frey filaments. The resulting stimulus-response curve was plotted and analyzed via non-linear regression analysis. EF<sub>50</sub> was calculated as the force at which animals show a 50% response rate.

**Conditioned place preference test.** To assess non-reflexive pain behaviors, the conditioned place preference (CPP) test was performed in automated chambers obtained from Harvard Apparatus (Model LE896-LE898, Holliston, MA, USA) placed inside of isolation cubicles

(Habitest Model H10-24TS, Coulbourn Instruments, Holliston, MA, USA). The apparatus consisted of three chambers; the middle transparent chamber and two conditioning chambers with striped walls and a smooth floor or dotted walls and a textured floor. Mice were habituated by allowing them to freely move between the three chambers for 45 min on day 5 post-inoculation. On days 6–8, mice were injected with vehicle and conditioned by immediately restricting them in one of the conditioning chambers for 1 h. Mice were then put back in their cages for 4 h followed by injection with the test drug and conditioned for 1 h in the other conditioning chamber. On day 9 post-inoculation testing was performed by allowing the animals to freely move between all three chambers for 45 min. Data are presented as CPP score,<sup>31</sup> measured as time spent in vehicle- or drug-paired chamber divided by total time spent in both conditioning chambers.

### Quantitative real time-PCR

The ipsilateral V3 region of the TG was collected from decapitated tumor-bearing and normal mice, in Qiazol reagent (Sigma, St. Louis, MO). Total RNA was extracted from tissues using RNeasy Mini Kit (Qiagen, Valencia, California, USA) as per manufacturer's instructions. Isolated RNA was then subjected to cDNA synthesis using Superscript III First Strand Synthesis kit (Invitrogen, CA, USA). Fixed amounts of cDNA were used as a template in the RT-PCR protocol. Amplification was detected using customized RT<sup>2</sup> Profiler PCR Array for mouse (Qiagen). The reactions were run in 25  $\mu$ l volume including GAPDH as an endogenous control. Data were acquired for five animals per group and quantified using comparative delta-delta Ct (ddCT), normalized to the data based on the endogenous reference.

### Statistics

Data are presented as mean  $\pm$  standard error of mean (SEM). Statistical analyses were performed using one- or two-way ANOVA with Bonferroni correction.  $P < 0.05$  was considered significant.

## Results

### *The in vivo orthotopic model of oral squamous cell cancer produces tumor growth in the tongue and reduces body weights in mice*

To produce an in vivo orthotopic oral tumor model, we used a modified version of the tongue cancer pain model developed by Schmidt and colleagues.<sup>13,19–21</sup> The OSCC cell line HSC2 was injected into the ventral tongue of

athymic mice and animals were monitored for tumor growth every two days (Figure 1). The control groups received either NOK cells into the tongue, the colon cancer cell line HT29 cells into the tongue, or HSC2 into the hindpaw. The HSC2 injected mice grew observable lingual tumors by day 6 post-inoculation that continued to grow for the entire two-week period. Figure 1(a) illustrates the in situ tumor growth at day 9 in HSC2 mice. The NOK cell-injected group had normal appearing tongues throughout the two-week period (Figure 1(b)). The HSC2 lingual tumor group had reduced body weights by day 6 that continued to decrease during the two-week period (Figure 1(e)). The mean body weights of the control groups were unaffected. The additional control groups of HT29 cells injected in the tongue and HSC2 cells injected in the paw showed observable tumors by day 6 (Figure 1(c) shown at day 9 post-inoculation) and day 14 (Figure 1(d)), respectively, and continued to maintain body weights through the study period (Figure 1(e)). Because mice injected with HSC2 into the hindpaw grew tumors later than other groups, their body weights were measured up to 24 days post-inoculation (Figure 1(e)). This finding emphasizes the importance of an orthotopic model as injection of the HSC2 cell line into the tongue produced significant and rapid loss in body weight compared to injection of the same cell line into the hindpaw.

### *In vivo orthotopic model of OSCC produces well-differentiated tumors with an immune response*

Histological examination of mouse tongues was performed nine days after injection of either NOK or HSC2 cell lines. As illustrated in Figure 2(a), tongues injected with NOK cells showed no noticeable histological changes and the normal architecture of the epidermal-muscular junction was preserved. In contrast, the tongues injected with HSC2 cells demonstrated a well-differentiated tumor infiltrating the muscles and surrounding tissues (Figure 2(b)). At higher magnification, an immune response to the tumor was evident as seen by infiltration of neutrophils, lymphocytes, and macrophages at the tumor-tongue junction (Figure 2(c)).

### *Immunohistochemical characterization of the orthotopic model*

Immunohistochemical analyses of tongue and TG tissues were performed in order to further characterize the orthotopic model. As compared to the control tongue tissue, the induction of HSC2 tumor resulted in increased expression of transmembrane protease serine 2 (TMPRSS2; Figure 3(a) and (b)), an enzyme previously reported to be expressed in OSCC tumors and associated with pain production.<sup>32</sup> TMPRSS2 was selectively expressed within the tumor cells, as indicated by

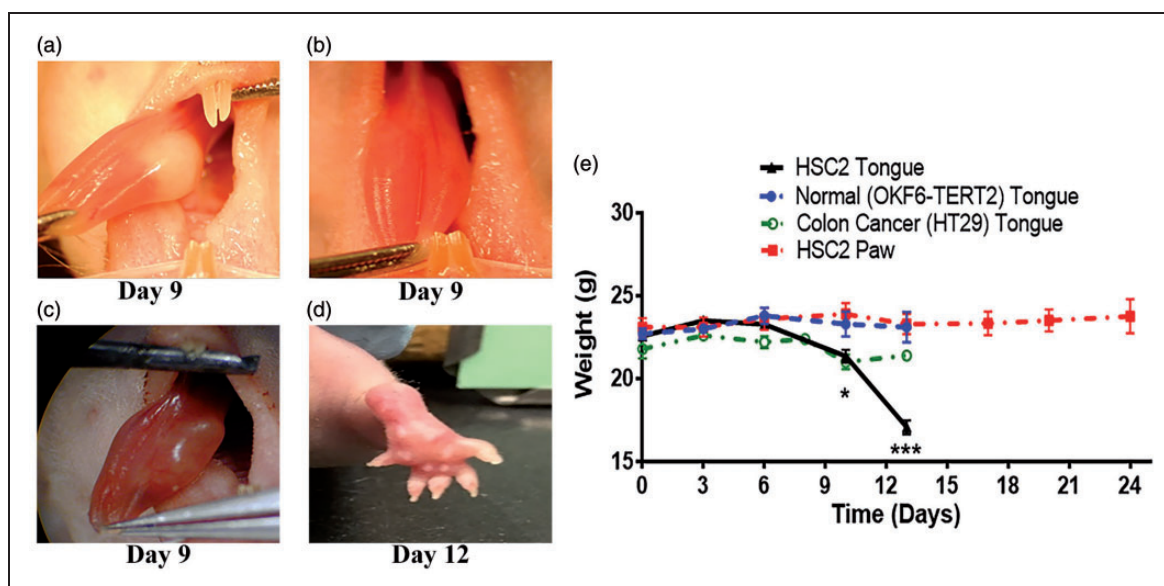


**Figure 1.** Effect of tumor injection in athymic mice on body weights. (a) Presentation of human OSCC cells, HSC2, after injection into the tongue of male nude mice. Visible tumor was observed by day 6, tumor growth shown at day 9. (b) Control mice injected with human NOK cell line; OKF6-TERT2 into the tongue (day 9). (c) Human colon cancer cells; HT29 injected in the tongue, tumor growth shown at day 9. (d) HSC2 cells injected into hind paw of an athymic mouse. Tumor growth shown at day 14. (e) Body weights of mice taken every three days post-inoculation for each group. Control groups include injection of normal cells, HSC2 cells into the paw or the HT29 colon cancer cell line into the tongue. N = 8–10/group. Data represented as mean  $\pm$  SEM and analyzed by ANOVA. \* $p < 0.05$  \*\*\* $p < 0.001$ .

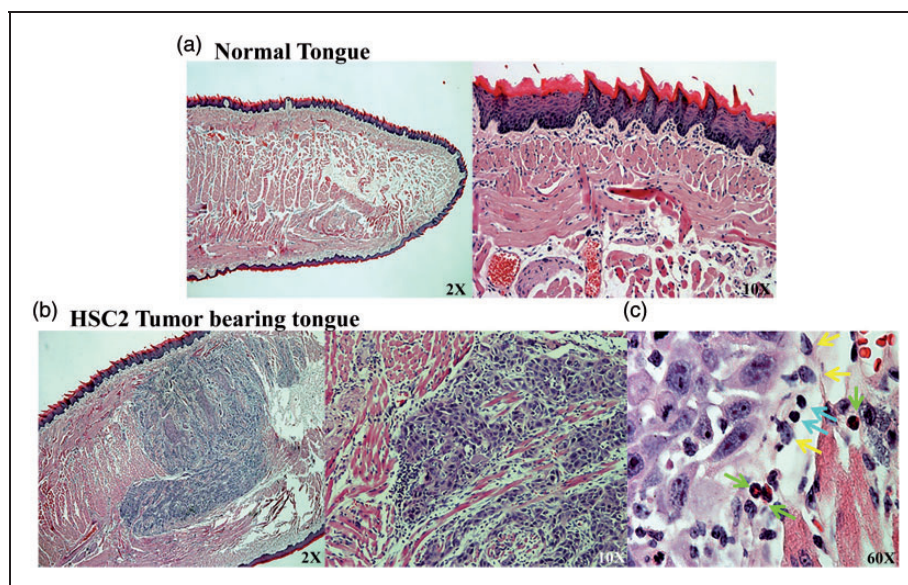


**Figure 2.** Histological characterization of normal and tumor-bearing tongue. Either  $3.5 \times 10^{-5}$  NOK cells (Panel a) or HSC2 cells (Panel b) were injected in tongue of athymic mice. At nine days post-inoculation, tongues were dissected, sectioned, and subjected to H&E staining. Panel c. Images taken at  $60 \times$  from HSC2-bearing tongue indicate an immune reaction upon tumor growth. Green arrows indicate neutrophils, cyan arrows indicate lymphocytes, and yellow arrows indicate macrophages.

co-localization with a human mitochondrial marker (Mito). In addition, the tumor appears to be well vascularized (Figure 3(f)) and innervated by peptidergic neurons (Figure 3(d)) and sympathetic fibers (Figure 3(j) and (h)) as seen by positive staining for CD31, von Willebrand Factor (vWf), and calcitonin-gene-related peptide (CGRP), and tyrosine hydroxylase (TH), respectively. Examination of the V3 region of the TG (Figure 3(i) and (j)) did not reveal a detectable up-regulation of ATF3 in tumor-bearing animals, suggesting that the tumor does not damage the lingual nerve.

#### *Orthotopic OSCC tumor model reduced food intake that is reversible by analgesics*

Oral cancer patients experience pain during chewing and swallowing.<sup>10,11</sup> Therefore, feeding behaviors of mice were measured to reflect this clinical symptom (Figure 4). Mice injected with NOK cells demonstrated no significant differences in the amount of food ingested over a two-week period, or after vehicle or drug (indomethacin, tramadol) administration (Figure 4(c) and (d)). Mice injected with HSC2 cells in the tongue had reduced food intake by day 7 that progressed over time. Interestingly, treatment with the NSAID indomethacin resulted in significantly greater feeding compared to vehicle injection at day 7 (Figure 4(a)). However, indomethacin was ineffective at later time points. In contrast, treatment with the opioid tramadol significantly increased the amount of food intake at day 9 as well as day 14 (Figure 4(b)). Morphine analgesia was

ineffective in maintaining food intake in HSC2 mice as it decreased amount of food ingested for all animals tested including controls. This finding is similar to previous studies reporting a decrease in feeding behavior with morphine in Balb/c mice.<sup>33</sup> To determine whether the reduction in food intake was due to nociception and not due to metabolic abnormalities from having a tumor in the body, we used a control group that received HSC2 cells in the paw. As shown in Figure 4(e) and (f), a tumor growing in the paw did not reduce food intake of mice at any given time point tested. Because we observed tumors in the paw only by day 14, feeding behavior of this group was monitored through day 25 post-inoculation, with no effects noted (Figure 4(f)). To determine whether the reduced feeding was due to OSCC tumors and not merely due to a cellular growth in the tongue, we injected a cell line (HT29) from a typically non-painful colon cancer, into the tongue. Despite the presence of a visibly growing tumor in the tongue, there was no reduction in food intake (Figure 4(g) and (h)). Taken together, these data suggest that orthotopic OSCC tumors in mice produce pain-like behaviors during feeding and mimics this important patient-reported symptom.

#### *OSCC tumor produces referred mechanical allodynia that is reversible by analgesics*

Mechanically evoked pain is a hallmark feature in oral cancer patients.<sup>10</sup> To evaluate this phenotype in mice, von Frey filaments were applied onto the vibrissal pad with assessment of escape behaviors. As shown in

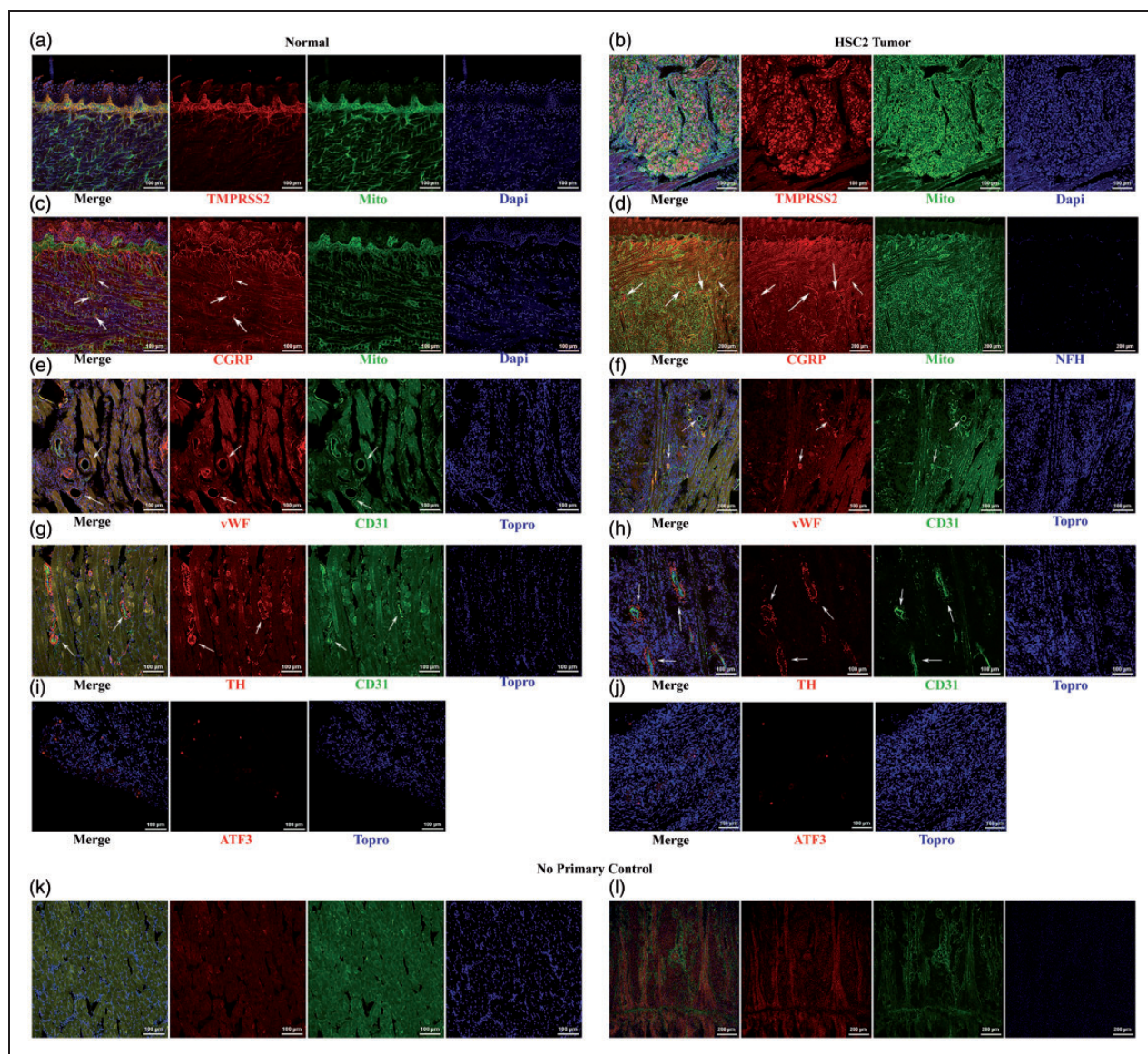


**Figure 3.** Immunohistochemical characterization of the orthotopic tumor model. Tissues were collected and characterized by immunohistochemical analysis at nine days after injection of NOK cell line (Left column of images) or HSC2 cell line (Right column of images). Panels a and b present TMPRSS2 and human mitochondria staining in NOK and HSC2-treated animals. Panels c and d illustrate CGRP and human mitochondrial marker Mito in NOK HSC2-treated animals. Arrows indicate CGRP positive fibers within and around the tumor. Panels e and f indicate expression of vWF and CD31 staining in NOK and HSC2 groups. Arrows indicate blood vessels within the tumor. Panels g and h present tyrosine hydroxylase (TH) and CD31 staining after NOK and HSC2 injections. Arrows indicate blood vessels and sympathetic fibers. Panels i and j illustrate ATF3 staining in the ipsilateral V3 region of the TG at day 9 post-inoculation of NOK or HSC2. k–l: No primary control with staining for secondary antibodies used for all the staining showed.

Figure 5(a), HSC2-injected mice exhibited a significantly decreased threshold to mechanical stimuli compared to the normal group, as demonstrated by a leftward shift of the stimulus-response curve with an approximate 4-fold reduction in  $EF_{50}$  (0.39 mN compared to 1.6 mN). This suggests that tumor growth in the mandibular V3 distribution (i.e., tongue) produces central plasticity and sensitization in the maxillary V2 region of the trigeminal nerve. In contrast, injection of the colon cancer cell

line HT29 did not produce a significant difference in mechanical thresholds (Figure 5(b)). The reduction in threshold of HSC2-injected mice was reversed by treatment with opioids such as morphine ( $EF_{50}$  increased by 2.5-fold to 0.88 mN compared to vehicle group  $EF_{50}$  0.39 mN) and tramadol ( $EF_{50}$  increased by 5-fold to 0.98 mN compared to vehicle group  $EF_{50}$  0.49 mN). The normal control group was unaffected by either drug (Figure 5(c) to (f)). Administration of

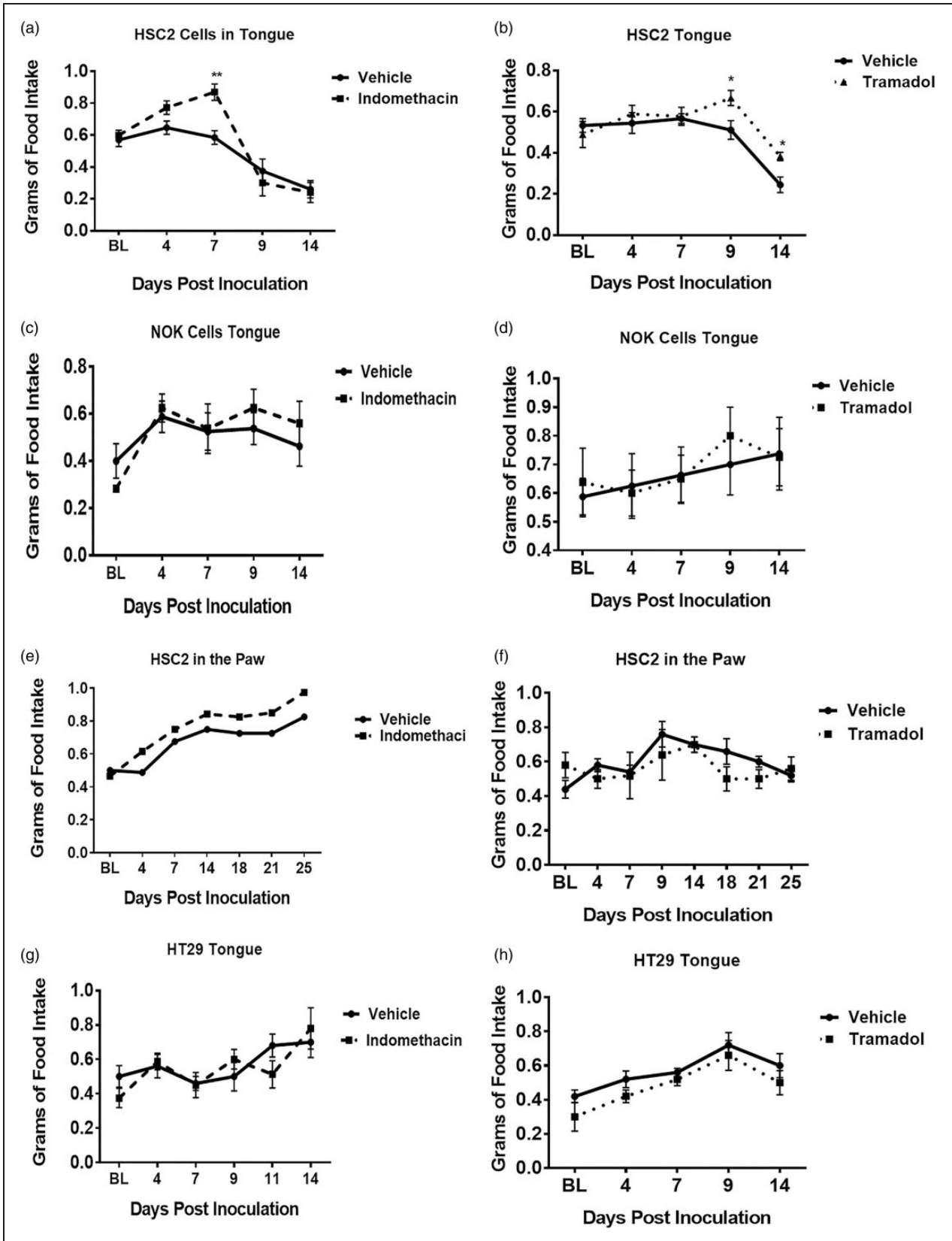


**Figure 4.** Effect of tumor development on feeding behavior in mice. Mice were tested every four days after tumor inoculation. Mice injected with HSC2 experienced a decrease in amount of food ingested by day 7 that was reversible with administration of

(continued)



indomethacin (5 mg/kg i.p.) did not affect mechanical thresholds of tumor-bearing or normal mice (data not shown), suggesting that prostaglandins may not be involved in mediating tumor-induced mechanical hypersensitivity.

### OSCC tumor in mice produces ongoing, spontaneous pain

Patients with OSCC tumors often report spontaneous pain,<sup>13</sup> and here we employed the CPP assay to evaluate

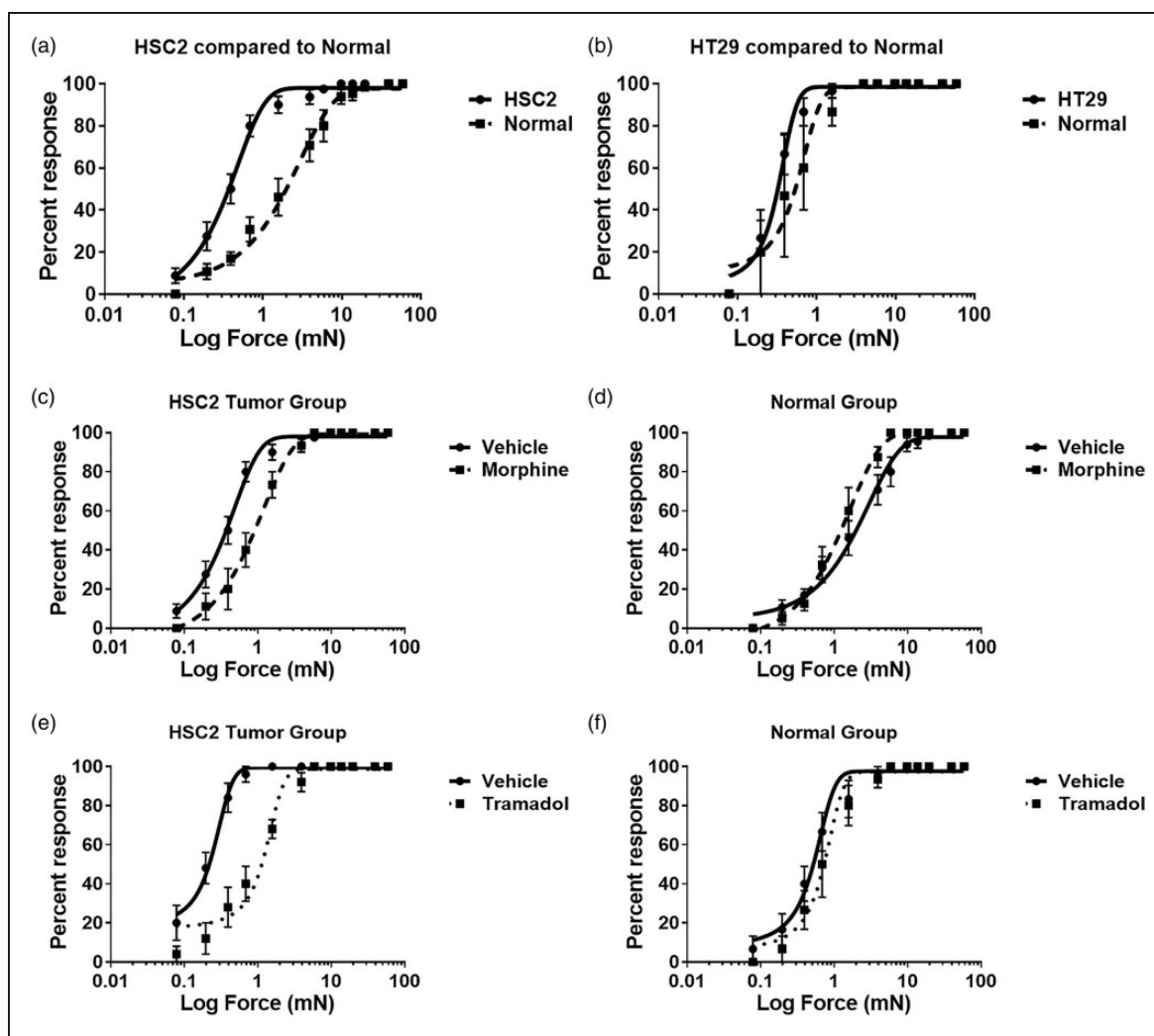


**Figure 5.** Effect of tumor injection into the V3 division of the TG (tongue) on mechanical allodynia in the V2 division (vibrissal pad). Mice were tested with von Frey filaments applied to the vibrissal pad with detection of escape responses at nine days after tumor injection. Data are plotted as % response to a series of five applications of a given filament. (a). Comparison of mice with an HSC2 tumor in the tongue compared to an untreated control group. (b) Evaluation of the effect of inoculation of the colon cancer cell line HT29 with untreated control mice. (c) Effect of treatment with morphine 3 mg/kg i.p. 30 min prior to testing in HSC2 tumor- or untreated control mice. (e) and (f) Effect of tramadol 20 mg/kg i.p. in HSC2 tumor (Panel e) or untreated control (Panel f) mice. Data are mean  $\pm$  SEM.  $n = 8-12$  per group.

#### Figure 4. Continued

(a) indomethacin 5 mg/kg i.p. and (b). tramadol 20 mg/kg i.p. (c) Control mice injected with NOK, (e) HSC2 cells in the paw and (g) colon cancer cells showed neither a decrease in amount of food ingested after vehicle injection nor an increase in food ingested after administration of indomethacin. (d) Control mice injected with NOK, (f). HSC2 cells in the paw and (h) colon cancer cells showed neither a decrease in amount of food ingested after vehicle injection nor an increase in food ingested after administration of tramadol. All injections were given 30 min prior to start of testing period. Data represented as mean  $\pm$  SEM and analyzed by two way ANOVA with  $p < 0.05$  as significant.  $n = 8-13$  per group.

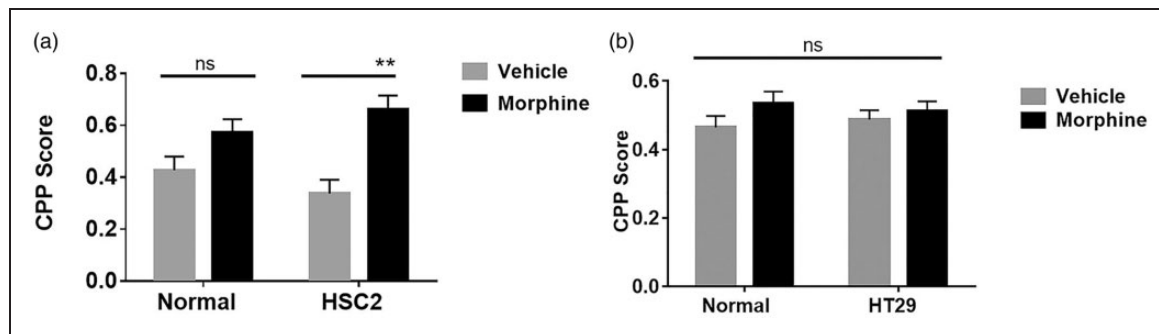


**Figure 6.** Effect of tumor injection on conditioned place preference (CPP) to morphine. Mice were injected with tumor into the tongue, habituated on day 5, conditioned with either a vehicle- or morphine-paired chamber for one hour on days 6–8 and tested for CPP on day 9. The CPP score is the ratio of time spent in drug- or vehicle-paired chamber/total time spent in both-chambers. (a) Mice injected with HSC2 spent significantly more time in the morphine 3 mg/kg i.p. paired chamber than the vehicle chamber. (b) Mice injected with non-pain producing colon cancer; HT29 cells spent no significant difference in amount of time spent in the morphine-paired chamber as the normal control mice. Data represented as mean  $\pm$  SEM and analyzed by two-way ANOVA with  $p < 0.05$  as significant.  $n = 12$ /group.

this component. As seen in Figure 6(a), when morphine is used as an analgesic, control (NOK) mice showed no preference between either the vehicle-paired chamber or the drug-paired chamber as observed by statistically insignificant CPP scores. However, HSC2 tumor-bearing mice exhibited a significant preference to the morphine-paired chamber suggesting that OSCC tumors produce ongoing pain in mice. Indomethacin treatment had no effect on CPP scores of either normal mice or HSC2 tumor-bearing mice (data not shown). Interestingly, we also performed CPP test between normal mice and mice bearing the HT29 tumor (Figure 6(b)), with no significant difference observed between the preference for the morphine-paired chamber between normal and colon tumor mice. These data suggest that OSCC tumors produce ongoing pain, whereas “non-painful cancers” in the tongue may not.

#### *Molecular characterization of TG in the orthotopic tumor model demonstrates alteration in expression of markers of the pain pathway*

Molecular characterization of the neuronal response to the orthotopic tongue cancer model was performed by evaluating changes in TG expression after tumor growth, of several genes known to be involved in activation of the pain pathway. Categories of evaluated genes included ion channels, G-protein coupled receptors, tyrosine kinase receptors, neurotransmitters and inflammatory mediators. As seen in Figure 7(a), several genes were either up-regulated or down-regulated in the V3 area of the TG tissue, after HSC2 tumor growth at day 9 compared to NOK-injected mice. Some of the genes that produced striking alteration in TG expression were up-regulation of brain-derived neurotrophic factor (BDNF, 100% increase compared to control, Figure 7(b)) and

sodium channel 1.3 (SCN3A, 87% increase compared to control, Figure 7(c)) and down regulation of tyrosine kinase A receptor (NTRK1, 60% decrease compared to control, Figure 7(d)).

#### *BDNF is up-regulated in TG neurons after tumor growth and contributes to pain-like behavior in HSC2 tumor-bearing mice*

To further characterize BDNF expression in the TG after tumor growth, immunohistological analysis of BDNF expression in TG neurons in normal and tumor-bearing animals was performed. As shown in Figure 8(a) to (c), BDNF was primarily expressed in neuronal cells of the TG tissue and demonstrated a significant increase in the total number of TG neurons in the V3 area of HSC2 tumor-bearing mice compared to the control group (Figure 8(d)). Figure 8(d) and (e) shows that BDNF is also expressed in the V2 region of TG tissue of normal and tumor-bearing group. These data indicate that induction of an OSCC leads to an increase in both; BDNF transcripts (Figure 7) and protein (Figure 8).

To determine whether BDNF signaling contributes to OSCC nociception, we administered the TrkB receptor antagonist, ANA-12, to untreated control and HSC2-treated animals. Mechanical evoked hypersensitivity thresholds were reversed in the ANA-12-treated tumor-bearing mice as observed by a 7-fold rightward shift in their response curve (0.67 mN after ANA-12 administration compared to 0.13 mN with vehicle; Figure 9(a)). In contrast, no difference was observed in normal controls (Figure 9(b)). In addition, ANA-12 treatment significantly increased feeding in HSC-treated animals (Figure 9(c)) but not the untreated control group (Figure 9(d)).

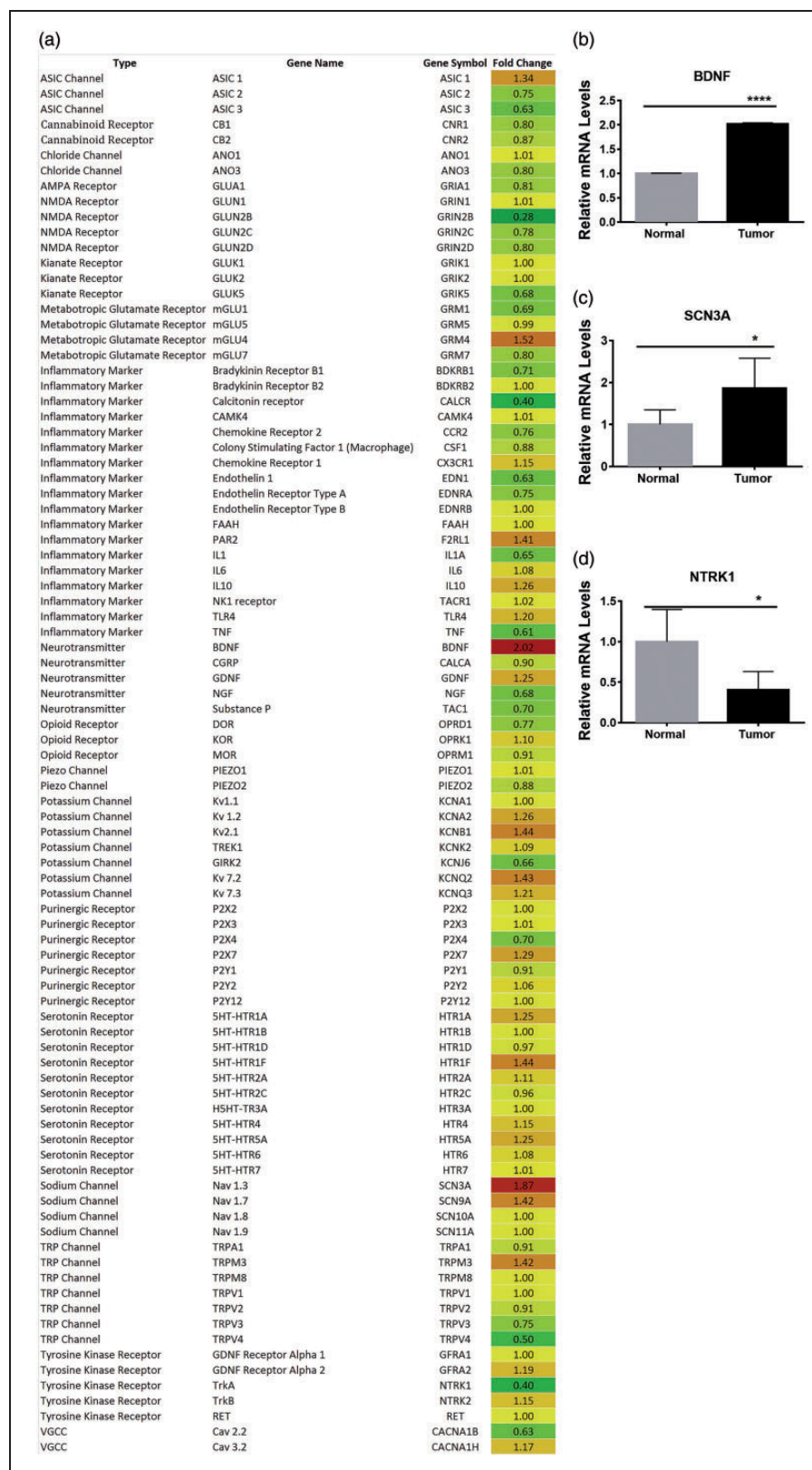


**Figure 7.** RT-PCR analysis of the V3 region of the ipsilateral trigeminal ganglion from normal and HSC2-bearing mice. (a) Mice were injected with NOK or HSC2 cells in the tongue and V3 region of ipsilateral TG were dissected at day 9 post-inoculation and subjected to RT-PCR array for known pain markers. N = 5 per group were used. Data represented as a heat map for expression levels of each gene for tumor-bearing group normalized to the normal group. Numbers within the heat map indicate fold difference between tumor-bearing and normal groups. (b) Individual quantification for representative genes modified after tumor growth is shown in (b). BDNF, C. SCN3A and D. NTRK1. Error bars = S.E.M. \**p* < 0.05 by t-test. N = 6 per group.

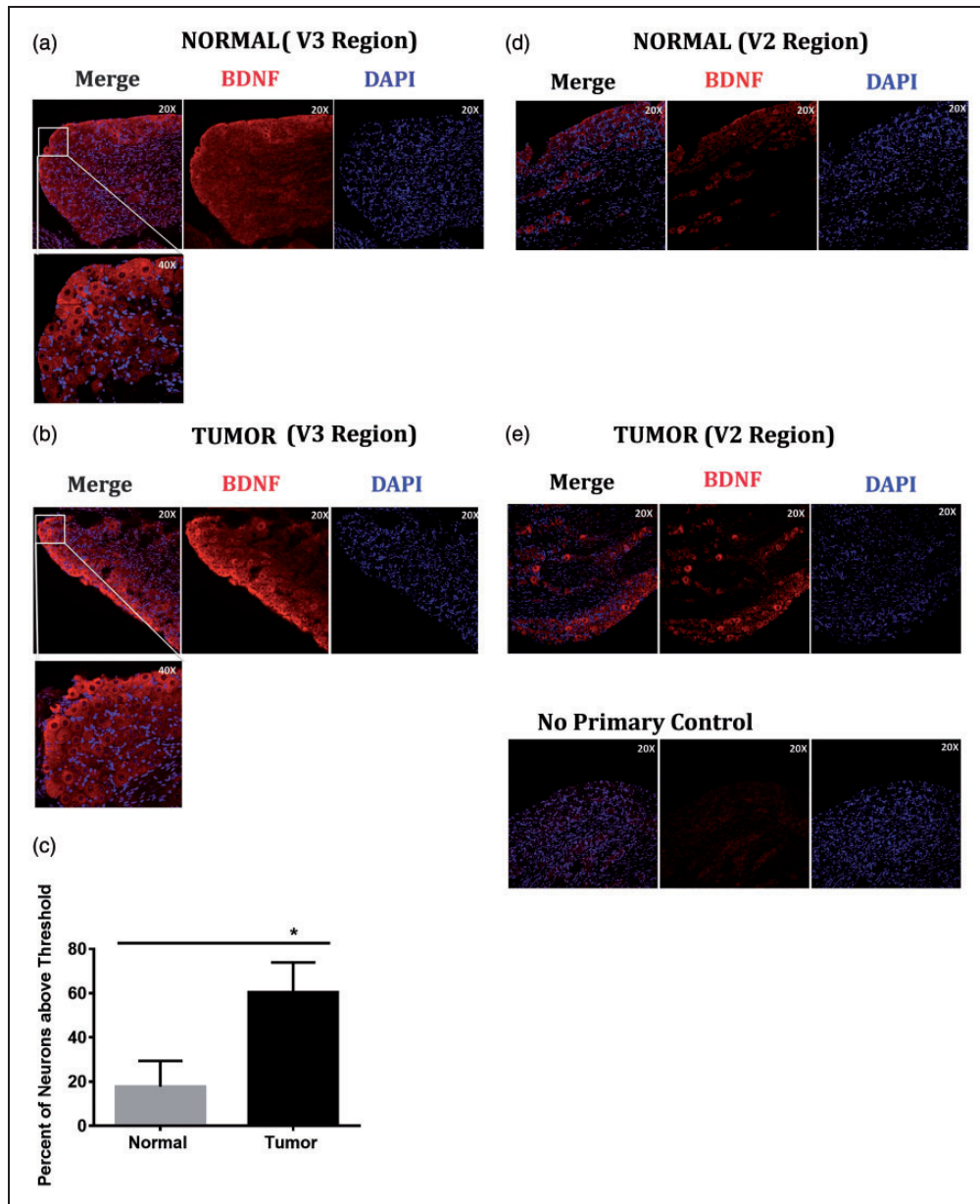


**Figure 8.** Elevation of BDNF in TG neurons after HSC2 administration to the tongue. At nine days after inoculation, the tongue was removed and processed for immunohistochemical staining for BDNF expression in the V2 and V3 region. Topro was used to reveal cellular nuclei. Mice were injected with either NOK cells (Panels a and d) or HSC2 cells (Panels b and e). (f) Images shown for 'no primary' Ab control. (c) Quantification of percentage of BDNF positive neurons in the V3 region of the ipsilateral TG from normal group and HSC2 tumor-bearing mice. N=4 per group. Data presented as mean  $\pm$  SEM.

## Discussion

Pain is an early, and often top ranked symptom in oral cancer patients that significantly reduces their quality of life.<sup>4,34,35</sup> Unlike other cancers, pain from oral cancer is produced at the primary site of the tumor even when the tumor is still quite small in size. This suggests that OSCC cells control the activity of nearby nociceptors. To systematically study mechanisms by which oral tumors produce pain, it is crucial to develop a well-characterized

animal model that reproduces the constellation of patient symptoms.

Previous studies by the Schmidt group and other groups have established this in vivo orthotopic model of OSCC pain.<sup>13,19–22</sup> Here, we have adapted this model and made three new findings. First, we demonstrate that this OSCC pain model engages higher order cognitive systems (CPP assay), in addition to the effects on feeding, weight gain, and mechanical allodynia referred to the V2 division. Second, this behavioral

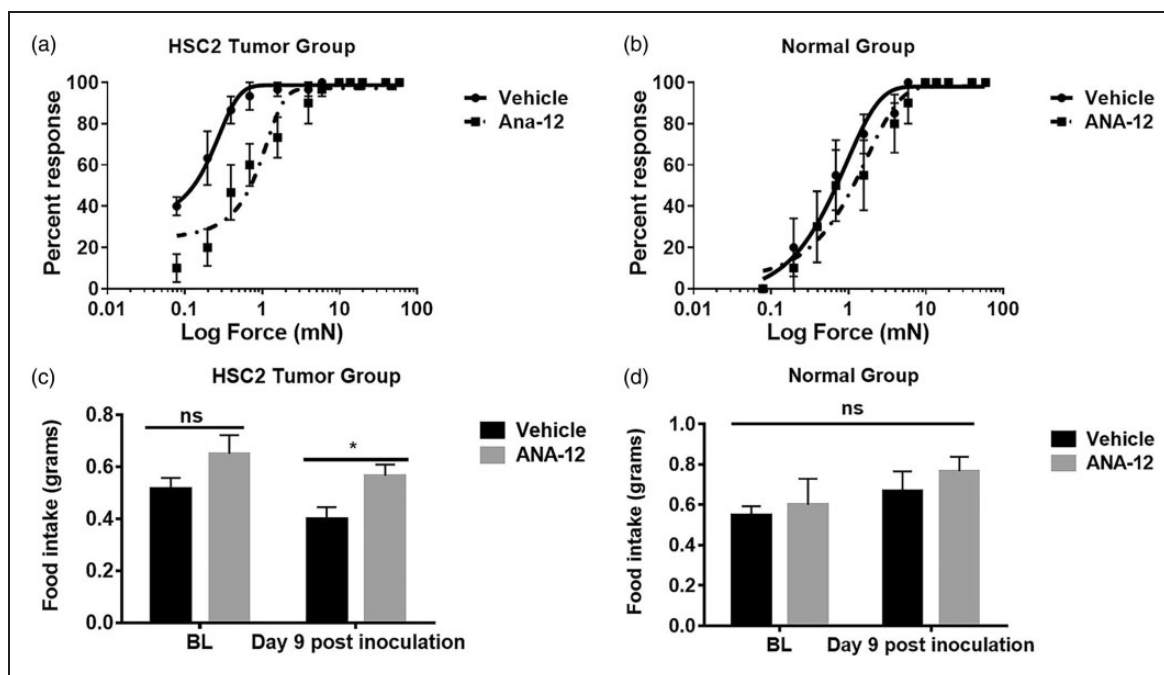


**Figure 9.** Effect of the TrkB antagonist, ANA12, on OSCC-evoked nociception. At nine days after inoculation with HSC2, animals were tested for mechanical allodynia in the vibrissal pad (Panels a, b) or for feeding (Panels c, d) using methods described in the legends to Figures 4 and 5. Mice were injected with either the TRKB antagonist ANA-12 1 mg/kg i.p. or vehicle. Error bars are S.E.M. \* $p < 0.05$ .  $n = 6$  per group/assay.

phenotype is specific to HSC2 injected into the tongue, it is not seen with HSC2 injected into the hindpaw, nor is it observed following injection of hNOK or human colonic cancer cells into the tongue. Thus, there is a critical tumor-tissue environment interaction that mediates OSCC pain. Third, we demonstrate a potential role of BDNF signaling in oral cancer pain.

We modified the previously developed tongue cancer pain model by using a well-characterized human OSCC cell line, HSC2 to grow the tongue tumor in male athymic mice. Male mice were used in the study as it has been implicated that prevalence of oral cancer pain is higher in males than females. Connelly et al.<sup>36</sup> reported that men experienced significantly higher levels of function-related pain than women. Cuffari et al.<sup>10</sup> reported that presence of pain as an initial symptom for oral cancer was more common in men than women. However, we note that this does not exclude the need for future studies using female mice. HSC2 cells were used in this model since: (1) it is established from a male patient with a floor of the mouth tumor;<sup>37</sup> (2) we previously have reported that in vitro culturing of HSC2 evokes the release of soluble factors that are capable of triggering spontaneous nociceptive behavior and thermal and mechanical allodynia after i.p. hindpaw injection;<sup>38</sup> (3) it produces 100% tumor expression, meaning that it produces tumor in the tongue or the paw in every single animal; and (4) it does not metastasize in mice,<sup>39,40</sup> which can be a

confounding factor in studying the role of OSCC cells in regulating nociceptor activity. Our data demonstrate that HSC2 cells produce a well-differentiated tumor by day 6 post-inoculation and was able to elicit an immune response as seen by infiltration of lymphocytes, neutrophils and macrophages (Figure 2(c)) suggesting that athymic mice were able to mount at least a partial immune response against the tumor, which is important as inflammation may in part contribute to the pain profile.<sup>41</sup> We do note, however, that athymic mice have a blunted T cell response and therefore this model does not address the role of T cell immunity in oral cancer pain.

Immunohistochemical analysis of tumor-bearing tongue revealed an up-regulation of TMPRSS2 (Figure 7(b)), a previously characterized marker for pain producing tumors such as OSCC.<sup>32</sup> Additionally, the tumor was well innervated with peptidergic afferent fibers and sympathetic fibers surrounding blood vessels (Figure 7(e) and (h)). However, there was no increase in ATF3 expression in TG sections (Figure 7(j)), suggesting that the tumor may not damage the lingual nerve. This observation is substantially different from bone cancer pain models,<sup>42</sup> further emphasizing the importance of using orthotopic tumor models.

Next, we optimized three behavioral assays designed to reflect the spectrum of cancer patient symptoms, including alterations in feeding,<sup>36</sup> referred facial pain,<sup>10</sup> and spontaneous pain.<sup>36</sup> As shown in Figure 4, mice with

HSC2 tumors exhibited significantly reduced food intake compared to normal mice by day 7 post-inoculation. The results indicated that this OSCC tumor model produced a reduction in feeding behaviors that was specific to both tumor type (HSC2 more effective than the colon cancer HT-29) and location (HSC2 in tongue vs hindpaw). In addition, this loss in feeding was reversed by a NSAID in early stages of development and by an opioid in later stages of tumor growth. These data emulate clinical recommendations by the World Health Organization step-ladder suggesting that NSAIDs be used initially followed by opioids when NSAIDs become refractory.<sup>43</sup> Taken together, these data illustrate two key features of the feeding behavior: (1) the reduction in feeding in HSC2 tumor-bearing mice is due to pain-like behaviors experienced by the animals during feeding and (2) this pain-like behavior is specific to OSCC tumor and not merely due to having a foreign mass in the oral cavity. Notably, weight loss in mice was observed only in mice with HSC2 tumor in the tongue and not with any other groups tested suggesting that reduction in body weight was possibly due to reduction in food intake by the HSC2 tumor-bearing animals (Figure 1(e)) and not due to metabolic changes from having a tumor in the body. We note that this feeding assay is supplementary to the gnawing behavior assay used previously<sup>19</sup> and while the latter specifically measures pain-like chewing behavior as seen in patients, one advantage of this feeding behavior assay is that it permits repeated measures of vehicle and drug on the same day in their home cages, substantially reducing the number of animals required for an experiment.

In addition to the feeding assay, we present two other behavioral assays for oral cancer pain not reported previously; (1) Von Frey test in the vibrissae to indicate facial pain and central sensitization and (2) Conditioned placed preference test to measure ongoing pain. To test referred facial pain, we probed a site within the V2 division of the TG (i.e., vibrissal pad) with graduated von Frey filaments in a manner similar to previous studies with neuropathic pain models.<sup>30</sup> The results demonstrated that HSC2 tumor growth produced significant reduction in mechanical thresholds compared to normal animals, suggesting referred V2 facial pain mediated by a tumor in the V3 division of the TG. This may be due to central plasticity within the medullary dorsal horn. Central sensitization through changes in the medullary dorsal horn has also been previously reported in a tongue cancer pain model as well as other facial cancer pain models.<sup>22,44</sup> Interestingly, the reduction in threshold was reversed by an opioid like morphine or tramadol (Figure 5(c) and (e)) but not by indomethacin. Again, the reduction in mechanical threshold was limited to HSC2 tumor animals and not observed in animals bearing colon cancer cell tumors.

With the CPP assay, we observed that HSC2 tumor-bearing animals significantly preferred the morphine-paired chamber compared to vehicle-paired chamber, whereas the normal mice preferred both chambers equally suggesting that HSC2 tumor in the tongue produced ongoing pain (Figure 6(a)). We did not observe a difference in preference with indomethacin treatment between normal and HSC2 tumor mice suggesting that inflammatory mediators and prostaglandins may not play a role in mediating OSCC-induced ongoing pain. Moreover, similar to the feeding behavior assay and Von Frey testing, CPP testing showed no difference between normal animals and colon cancer cell tumor-bearing mice (Figure 6(b)). This finding indicates that even though the environment and extracellular matrix is the same, differences in cancer cell types can produce a significant difference in the pain phenotype. Conversely, altering the growth environment can also change the dynamics of tumor growth and regulation, the time taken to observe a visible HSC2 tumor in the paw is longer than the time taken for the same cells to grow in the tongue. Further, the sensory innervation and the interaction of the tumor cells with the surrounding nociceptors can be different in various tissues. Collectively, these findings reinforce prior conclusions<sup>19–21,27</sup> on the importance of employing orthotopic tumor models to conduct mechanistic and pharmacological studies for cancer pain.

Molecular characterization of the TG after tumor induction revealed changes in expression of several markers of the pain pathway including BDNF, SCN3A1, ASIC1, mGLU7, PAR2, IL10, Kv2.1, Kv7.2, 5HT-HTR1F, and TRPM3 (Figure 7(a)). The role of Nav1.3 up-regulation in V3 TG upon tumor growth is yet to be explored. To date, there is no evidence for its role in cancer pain, however, its role has been implicated in neuropathic pain, as its expression has been shown to increase in sensory neurons after peripheral nerve and spinal cord injuries.<sup>45,46</sup> Surprisingly, in our study, Nav1.3 expression was up-regulated even in the apparent absence of lingual nerve damage (i.e., no change in ATF3 expression) upon tumor growth. Further investigation for its role in oral cancer pain is warranted.

However, the most striking change in gene expression upon tumor growth was that of the brain-derived neurotrophic factor (Figure 7(a) and (b)). Our results revealed an increase in both BDNF transcripts and protein in TG neurons (Figure 8). We also observed that treatment with a TrkB antagonist significantly reversed tumor-induced facial pain as well as reduction in feeding (Figure 9(a) to (d)). Prior studies have implicated BDNF in mediating inflammatory and neuropathic pain,<sup>47</sup> as well as bone cancer pain models.<sup>48,49</sup> To our knowledge, this is the first study implicating a role of BDNF in OSCC evoked pain, with demonstration of a

significant reduction in both mechanical hypersensitivity and reduced eating behaviors. The fact that ANA12 treatment reversed von Frey thresholds in the face, suggests that BDNF signaling may be implicated in central sensitization either through up-regulation of its expression in the V2 TG neurons or post-synaptic changes in the medullary dorsal horn. Several reports have indicated that BDNF plays a key role in central modulation of pain, acting through post-synaptic TrkB receptors that trigger intracellular signaling cascades leading to central sensitization.<sup>48,50,51</sup> However, our data does not rule out a peripheral role of BDNF/TrkB signaling in OSCC pain. Interestingly, BDNF/TrkB axis has been reported to be overexpressed in head and neck tumors<sup>23</sup> and has been implicated in preventing apoptosis of HNC,<sup>25</sup> altering EMT<sup>23</sup> as well as conferring chemoresistance.<sup>52</sup> It is therefore possible that increased BDNF/TrkB levels in OSCC tumors can regulate peripheral nociceptors at the site of the tumor. Further studies are warranted to determine the cellular signaling mechanisms triggering BDNF/TrkB-induced tongue cancer pain. Notably, reports of PAR2 involvement has been reported in mediating BDNF-induced pain states,<sup>48,50</sup> has been shown to contribute to oral cancer pain<sup>27</sup> and has an elevated expression in our orthotopic model (Figure 7(a)). Even though other downstream targets of BDNF signaling such as NMDA receptors, and NGF and TrkA receptors<sup>49,50,53</sup> were either unaltered or down-regulated in TG neurons upon tumor growth, they cannot be ruled out for their role in BDNF-mediated postsynaptic regulation in dorsal horn neurons.

### Acknowledgements

We would like to thank Dr. Mayur Patil for his technical assistance for the immunohistological studies and perfusion of animals.

### Authors' contributions

LC developed CPP and Vonfrey Assay, conducted some immunohistochemistry experiments, analyzed data as well as wrote the manuscript. BS and VV developed and performed all feeding behavior assays. LC and MS carried out cell culture work and performed all injections in the tongue. MH helped with design of immunohistological experiments as well as analyses. SR designed and analyzed all experiments as well as edited the manuscript.

### Declaration of Conflicting Interests

The author(s) declared no potential conflicts of interest with respect to the research, authorship, and/or publication of this article.

### Funding

The author(s) disclosed receipt of the following financial support for the research, authorship, and/or publication of this

article: This study was supported by funds provided by the Palliative Care Pilot Award by the American Cancer Society (SR) as well as the Ella and Williams Owens Foundation Award (SR).

### References

- Rivera C and Venegas B. Histological and molecular aspects of oral squamous cell carcinoma (Review). *Oncol Lett* 2014; 8: 7–11.
- Neville BW and Day TA. Oral cancer and precancerous lesions. *CA Cancer J Clin* 2002; 52: 195–215.
- Pearman TP, Beaumont JL, Paul D, et al. Evaluation of treatment- and disease-related symptoms in advanced head and neck cancer: validation of the national comprehensive cancer network-functional assessment of cancer therapy-head and neck cancer symptom index-22 (NFNHSI-22). *J Pain Symptom Manage* 2013; 46: 113–120.
- Reyes-Gibby CC, Anderson KO, Merriman KW, et al. Survival patterns in squamous cell carcinoma of the head and neck: pain as an independent prognostic factor for survival. *J Pain* 2014; 15: 1015–1022.
- Saxena A, Gnanasekaran N and Andley M. An epidemiological study of prevalence of pain in head & neck cancers. *Indian J Med Res* 1995; 102: 28–33.
- Epstein JB and Stewart KH. Radiation therapy and pain in patients with head and neck cancer. *Eur J Cancer Part B Oral Oncol* 1993; 29B: 191–199.
- van den Beuken-van Everdingen MH, de Rijke JM, Kessels AG, et al. Prevalence of pain in patients with cancer: a systematic review of the past 40 years. *Ann Oncol* 2007; 18: 1437–1449.
- Jain PN, Pai K and Chatterjee AS. The prevalence of severe pain, its etiopathological characteristics and treatment profile of patients referred to a tertiary cancer care pain clinic. *Indian J Palliat Care* 2015; 21: 148–151.
- Hargreaves KM. Orofacial pain. *Pain* 2011; 152(3 Suppl): S25–S32.
- Cuffari L, Tesseroli de Siqueira JT, Nembr K, et al. Pain complaint as the first symptom of oral cancer: a descriptive study. *Oral Surg Oral Med Oral Pathol Oral Radiol Endod* 2006; 102: 56–61.
- Grond S, Zech D, Diefenbach C, et al. Assessment of cancer pain: a prospective evaluation in 2266 cancer patients referred to a pain service. *Pain* 1996; 64: 107–114.
- Keefe FJ, Manuel G, Brantley A, et al. Pain in the head and neck cancer patient: changes over treatment. *Head Neck Surg* 1986; 8: 169–176.
- Lam DK and Schmidt BL. Orofacial pain onset predicts transition to head and neck cancer. *Pain* 2011; 152: 1206–1209.
- Nagamine K, Ozaki N, Shinoda M, et al. Mechanical allodynia and thermal hyperalgesia induced by experimental squamous cell carcinoma of the lower gingiva in rats. *J Pain* 2006; 7: 659–670.
- Viet CT and Schmidt BL. Biologic mechanisms of oral cancer pain and implications for clinical therapy. *J Dent Res* 2012; 91: 447–453.

16. Dios PD and Leston JS. Oral cancer pain. *Oral Oncology* 2010; 46: 448–451.
17. Mercadante S, Dardanoni G, Salvaggio L, et al. Monitoring of opioid therapy in advanced cancer pain patients. *J Pain Symptom Manage* 1997; 13: 204–212.
18. Leemans CR, Braakhuis BJ and Brakenhoff RH. The molecular biology of head and neck cancer. *Nat Rev Cancer* 2011; 11: 9–22.
19. Dolan JC, Lam DK, Achdjian SH, et al. The dolognawmeter: a novel instrument and assay to quantify nociception in rodent models of orofacial pain. *J Neurosci Meth* 2010; 187: 207–215.
20. Ye Y, Dang D, Zhang J, et al. Nerve growth factor links oral cancer progression, pain, and cachexia. *Mol Cancer Therapeut* 2011; 10: 1667–1676.
21. Ye Y, Ono K, Bernabe DG, et al. Adenosine triphosphate drives head and neck cancer pain through P2X2/3 heterotrimers. *Acta Neuropathol Commun* 2014; 2: 62.
22. Tamagawa T, Shinoda M, Honda K, et al. Involvement of microglial P2Y12 signaling in tongue cancer pain. *J Dent Res* 2016; 95(10): 1176–1182.
23. Kupferman ME, Jiffar T, El-Naggar A, et al. TrkB induces EMT and has a key role in invasion of head and neck squamous cell carcinoma. *Oncogene* 2010; 29: 2047–2059.
24. Lee J, Jiffar T and Kupferman ME. A novel role for BDNF-TrkB in the regulation of chemotherapy resistance in head and neck squamous cell carcinoma. *PLoS One* 2012; 7: e30246.
25. Zhu L, Werner JA and Mandic R. Implications of tropomyosin-related kinase B (TrkB) in head and neck cancer. *Anticancer Res* 2007; 27: 3121–3126.
26. Liang DY, Sun Y, Shi XY, et al. Epigenetic regulation of spinal cord gene expression controls opioid-induced hyperalgesia. *Mol Pain* 2014; 10: 59.
27. Lam DK, Dang D, Zhang J, et al. Novel animal models of acute and chronic cancer pain: a pivotal role for PAR2. *J Neurosci* 2012; 32: 14178–14183.
28. Ramos DM, But M, Regezi J, et al. Expression of integrin beta 6 enhances invasive behavior in oral squamous cell carcinoma. *Matrix Biol* 2002; 21: 297–307.
29. Henry MA, Freking AR, Johnson LR, et al. Increased sodium channel immunofluorescence at myelinated and demyelinated sites following an inflammatory and partial axotomy lesion of the rat infraorbital nerve. *Pain* 2006; 124: 222–233.
30. Wei F, Guo W, Zou S, et al. Supraspinal glial-neuronal interactions contribute to descending pain facilitation. *J Neurosci* 2008; 28: 10482–10495.
31. Cunningham CL, Gremel CM and Groblewski PA. Drug-induced conditioned place preference and aversion in mice. *Nat Protoc* 2006; 1: 1662–1670.
32. Lam DK, Dang D, Flynn AN, et al. TMPRSS2, a novel membrane-anchored mediator in cancer pain. *Pain* 2015; 156: 923–930.
33. MARRAZZI MA, McQuarters A, Barnes C, et al. Male/female comparison of morphine effect on food intake – relation to anorexia nervosa. *Pharmacol Biochem Behav* 1996; 53: 433–435.
34. Ferrell BR. The impact of pain on quality of life. A decade of research. *Nurs Clin North Am* 1995; 30: 609–624.
35. Oliveira KG, von Zeidler SV, Podesta JR, et al. Influence of pain severity on the quality of life in patients with head and neck cancer before antineoplastic therapy. *BMC Cancer* 2014; 14: 39.
36. Connelly ST and Schmidt BL. Evaluation of pain in patients with oral squamous cell carcinoma. *J Pain* 2004; 5: 505–510.
37. Michi Y, Morita I, Amagasa T, et al. Human oral squamous cell carcinoma cell lines promote angiogenesis via expression of vascular endothelial growth factor and upregulation of KDR/flk-1 expression in endothelial cells. *Oral Oncol* 2000; 36: 81–88.
38. Ruparel S, Bendele M, Wallace A, et al. Released lipids regulate transient receptor potential channel (TRP)-dependent oral cancer pain. *Mol Pain* 2015; 11: 30.
39. Momose F, Araida T, Negishi A, et al. Variant sublines with different metastatic potentials selected in nude mice from human oral squamous cell carcinomas. *J Oral Pathol Med* 1989; 18: 391–395.
40. Takahashi H, Shigeta T, Umeda M, et al. A new in vitro invasion model for oral cancer using an acellular allogenic dermal matrix (Alloderm): the relationship among in vitro invasion activity, in vivo invasion and metastasis. *Kobe J Med Sci* 2011; 57: E128–E136.
41. Rao SK, Pavicevic Z, Du Z, et al. Pro-inflammatory genes as biomarkers and therapeutic targets in oral squamous cell carcinoma. *J Biol Chem* 2010; 285: 32512–32521.
42. Peters CM, Ghilardi JR, Keyser CP, et al. Tumor-induced injury of primary afferent sensory nerve fibers in bone cancer pain. *Exp Neurol* 2005; 193: 85–100.
43. Cleary J, Gelband H and Wagner J. Cancer pain relief. In: Gelband H, Jha P, Sankaranarayanan R, et al. (eds) *Cancer: disease control priorities*. 3rd ed. (Volume 3). Washington (DC): The International Bank for Reconstruction and Development/The World Bank, 2015.
44. Hidaka K, Ono K, Harano N, et al. Central glial activation mediates cancer-induced pain in a rat facial cancer model. *Neuroscience* 2011; 180: 334–343.
45. Wood JN, Boorman JP, Okuse K, et al. Voltage-gated sodium channels and pain pathways. *J Neurobiol* 2004; 61: 55–71.
46. Lindia JA, Kohler MG, Martin WJ, et al. Relationship between sodium channel NaV1.3 expression and neuropathic pain behavior in rats. *Pain* 2005; 117: 145–153.
47. Obata K and Noguchi K. BDNF in sensory neurons and chronic pain. *Neurosci Res* 2006; 55: 1–10.
48. Bao Y, Hou W, Liu R, et al. PAR2-mediated upregulation of BDNF contributes to central sensitization in bone cancer pain. *Mol Pain* 2014; 10: 28.
49. Tomotsuka N, Kaku R, Obata N, et al. Up-regulation of brain-derived neurotrophic factor in the dorsal root ganglion of the rat bone cancer pain model. *J Pain Res* 2014; 7: 415–423.
50. Tillu DV, Hassler SN, Burgos-Vega CC, et al. Protease-activated receptor 2 activation is sufficient to



- induce the transition to a chronic pain state. *Pain* 2015; 156: 859–867.
51. Constandil L, Goich M, Hernandez A, et al. Cyclotraxin-B, a new TrkB antagonist, and glial blockade by propentofylline, equally prevent and reverse cold allodynia induced by BDNF or partial infraorbital nerve constriction in mice. *J Pain* 2012; 13: 579–589.
  52. Lee M, Choy WC and Abid MR. Direct sensing of endothelial oxidants by vascular endothelial growth factor receptor-2 and c-Src. *PLoS One* 2011; 6: e28454.
  53. Kerr BJ, Bradbury EJ, Bennett DL, et al. Brain-derived neurotrophic factor modulates nociceptive sensory inputs and NMDA-evoked responses in the rat spinal cord. *J Neurosci* 1999; 19: 5138–5148.